X-ray Absorption Spectroscopy Study of $Cu_{0.25}V_2O_5$ and $Zn_{0.25}V_2O_5$ Aerogel-Like Cathodes for Lithium Batteries

Elisa Frabetti, Gregg A. Deluga, and William H. Smyrl*

Department of Chemical Engineering and Materials Science, University of Minnesota, 421 Washington Avenue S.E., Minneapolis, Minnesota 55455

Marco Giorgetti and Mario Berrettoni

Department of Physical and Inorganic Chemistry, University of Bologna and Unità di Ricerca INSTM di Bologna, Viale Risorgimento 4, 40136 Bologna, Italy

Received: December 1, 2003

Vanadium pentoxide materials prepared through sol−gel processes (xerogel, aerogel, and aerogel-like) act as excellent intercalation hosts for lithium as well as polyvalent cations. The large lithium insertion capacity of these materials makes them attractive for use as cathodes in high-capacity lithium batteries. The local structural modifications resulting from low dopant concentration (copper and zinc) in V_2O_5 aerogel-like material have been investigated by X-ray absorption spectroscopy (XAS). To study the structural sites of the polyvalent ions, extended X-ray absorption fine structure (EXAFS) spectra have been recorded at the vanadium, zinc, and copper K edges. The EXAFS analysis shows that the vanadium atomic environment is almost the same for $Cu_{0.25}V_2O_5$ and $Zn_{0.25}V_2O_5$. Furthermore, the doping metals (Cu and Zn) are found to be in the same site. Copper and zinc are 4-fold coordinated by almost-coplanar oxygens. This suggests a preferred site for the doping metal (M) and the same interaction between the vanadium and the doping metals. M−O first-shell distances are shorter for the copper compared to those for the zinc, and we have found higher disorder in the $Zn_{0.25}V_2O_5$ compound compared to that in $Cu_{0.25}V_2O_5$. No interactions between metal−metal sites were found because the metal doping level was too small.

Introduction

Many vanadium pentoxide gels have been synthesized during the last two decades via facile sol−gel chemistry[1] or hydrothermal methods.[2] A common method for the sol−gel preparation of vanadium oxide consists of the acidification of sodium metavanadate solution using an ion-exchange resin. The liquid obtained is then called hydrogel.[1] Xerogel (XRG) is produced by direct drying of the hydrogel.[3] Aerogels (ARG) were obtained by exchanging the water for acetone and then by supercritical drying of the hydrogel.[4] Amorphous vanadium oxide XRG and ARG are reported to have a higher storage capacity than the crystalline analogue when they are used as the cathode in lithium rechargeable batteries. The former can easily accommodate and release 4 equiv of lithium per mol of V_2O_5.[3] The latter is reported to intercalate up to 5.4 equiv of lithium per mol of V_2O_5 by chemical lithiation.[4] This high capacity has been ascribed to the amorphous structure, high porosity, high surface area, and small diffusion distances in the solid that must be penetrated by the guest ions. The Li^+ electrochemical intercalation rate is limited by diffusion in the host solid and not by the surface injection rate over a large range of rates. Short diffusion paths lead to a rapid insertion and release of guest species. The intercalation properties of V_2O_5 ARGs have been extended to polyvalent cations such as Al^{3+}, Zn^{2+}, and Mg^{2+}, and this shows the versatility of the host.[5] All of the polyvalent materials were produced by chemical insertion using the appropriate organometallic reagent.

Recently, it was found that to improve the properties of the materials, vanadium oxide in the hydrogel form could be doped with a metal by simple reaction with a known amount of the doping metal (copper, silver, zinc, nickel, and aluminum).[6] For example, copper doping yields higher electronic conductivity, a high insertion rate, and surprising long-term cyclability.[7] The synthesis is a multistep process based on a sequence of organic solvent exchange steps at near-ambient conditions, and the material produced, called aerogel-like (ARG-like), is highly porous and is characterized by a morphology extremely similar to that of ARGs.[7,8]

To gain a more complete understanding of the insertion chemistry of V_2O_5 materials and their use as intercalation electrodes in lithium battery systems, additional studies are required. A fundamental question is related to the nature of the intercalation sites: the electrochemical behavior suggests that some species are located in immobile sites (such as Cu^{2+} and Ag^+) and others, in mobile sites (such as Li^+, Mg^{2+}, and Zn^{2+}). Another issue related to the chemistry of intercalation is whether the preferred site is related to the nature of the cation or depends on the route of synthesis or maybe both. In this context, structural studies of the intercalation site in V_2O_5 have become the focus. X-ray absorption spectroscopy (XAS), which allows short-range structure investigation, was successfully used and demonstrated to be very useful.[9−11] Previous studies by XAS techniques on V_2O_5-based compounds allowed us to determine fundamental structural information on a variety of native and doped V_2O_5 compounds[12−17] using both ex-situ and in-situ techniques. In particular, the characterization of a zinc-

* To whom correspondence should be addressed. E-mail: smyrl001@tc.umn.edu.

10.1021/jp037656+ CCC: $27.50
Published on Web 03/02/2004

intercalated V_2O_5 ARG has shown a new and unconventional site for the guest ion; the Zn^{2+} ions are located within a single V_2O_5 layer, leaving the interlayer available for further ion insertion.[12] The zinc was chemically inserted into pristine ARG material. Also, in-situ XAS investigations of copper-doped V_2O_5 XRG indicate that the lithiation of this cathode proceeds with the concurrent formation of copper metal.[15] Thus, the copper was not lost to the solution during the cycle upon the insertion of lithium. The copper in the XRG materials seems to occupy an immobile site.

The present paper deals with the identification of the sites occupied by the guest metal (M) in $M_{0.25}V_2O_5$ ARG-like materials. The metal guests used in this study were copper and zinc. This is the first time in which the metallic site is investigated in homologous $M_xV_2O_5$ gel materials. The reason that we have started the investigation with the copper and zinc resides in the importance of this material as a very promising cathode for secondary lithium batteries. The materials investigated here were synthesized by a different route from that of the V_2O_5 gel materials analyzed previously. The presence of the guest doping metals allows the investigation of the zinc and copper K edges and provides structural information about the neighborhood of the inserted metals. Also, the study includes the data analysis of the measurements at the vanadium K edge for both samples, offering additional details of the local structure of the ARG-like host materials. A comparison of the two doped materials is also given, offering new insight into the nature of the preferred site for the guest metal. Finally, a comparison of the $Zn_{0.25}V_2O_5$ ARG-like material with a previous material with the same composition that was produced via a different synthesis route is also reported.

Experimental Section

Synthesis. Vanadium pentoxide hydrogels were synthesized by an ion-exchange process with sodium metavanadate.[3] The copper- and zinc-doped V_2O_5 ARG-like materials were prepared as described earlier by Coustier et al.,[6] except for modifications that were adopted to facilitate gel preparation with high metal concentration. Briefly, the doping was performed by mixing the selected stoichiometric amount of copper or zinc powder (ALFA 99.997% purity) with the V_2O_5 hydrogel. After the reaction was complete, the samples were dried under vacuum for several days. XRD powder spectra were taken on the dry, doped material. The absence of peaks associated with metallic copper or zinc clearly indicated that the reaction was complete.

XAS Data Collection. Samples for the XAS experiments were mixed with boron nitride and then were pressed as pellets (3 tons). X-ray absorption experiments were performed at the Synchrotron Radiation Source (SRS) at Daresbury Laboratory, Warrington, England, using beam line 7.1. The storage ring operates at 1.6 GeV and a typical current of 240 mA. Internal references for energy calibration were used for vanadium, zinc, and copper. Harmonics were rejected by detuning (80%). Data were acquired in transmission mode. Extended X-ray absorption spectroscopy (EXAFS) spectra were collected up to $k = 15$ every 0.03 k with a 3-s integration time (zinc and copper K edges) and up to to $k = 12$ every 0.03 k for 3 s (vanadium K edge).

XAS Data Analysis. The EXAFS analysis has been performed by using the GNXAS package[18,19] that takes into account multiple scattering (MS) theory. The method is based on the decomposition of the EXAFS signals into a sum of several contributions, the *n*-body terms. It allows the direct comparison of the raw experimental data with a model theoretical signal. The procedure avoids any filtering of the data and allows a statistical analysis of the results. The theoretical signal is calculated ab initio and contains the relevant two-body $\gamma^{(2)}$ and three-body $\gamma^{(3)}$ multiple scattering (MS) terms. The two-body terms are associated with pairs of atoms and probe their distances and variances. The three-body terms are associated with triplets of atoms and probe angles and bond−bond and bond-angle correlations. If useful, a single effective MS signal $\eta^{(3)}$ that includes both $\gamma^{(2)}$ and the $\gamma^{(3)}$ contributions can be used for the shells beyond the second one by using the same three-atom coordinates both for the two-atom and the three-atom contributions. The full definition of the parameters associated with the triplet of atoms is found in ref 18. Data analysis is performed by minimizing a χ^2-like function that compares the theoretical model to the experimental signal.

The phase shifts for the photoabsorber and backscatterer atoms were calculated ab initio starting from the structural model appearing in refs 12 and 20. They were calculated according to the muffin-tin approximation. The Hedin−Lundqvist complex potential[21] was used for the exchange-correlation potential of the excited state. Hereafter in the analysis, the starting signals have been successively recalculated to account for any important structural variation from the starting model. The core-hole lifetime, Γ_c, was fixed to the tabulated value[22] and included in the phase-shift calculation. The experimental resolution used in the fitting analysis was about 2 eV, in agreement with the stated value for the beamline used. To evaluate the effect of the structural disorder, the simulation was done by considering a non-Gaussian type of pair distribution functions. In fact, because of the amorphous nature of the compound, a more flexible model that replaces the simple Gaussian function might be expected to be required. The gamma-like (Γ) distribution has been used here[23,24] and has been proven to be very useful in previously studied systems.[25,26] The function depends on three parameters: the average bond distance, the bond variance, and the asymmetry coefficient (skewness) β defined as K_3/σ^3, where K_3 is the third cumulant of the distribution. The full definition of the function is described in refs 23 and 24.

Results

Structural studies of the intercalation site in the doped V_2O_5 ARG-like material were performed by extended X-ray absorption spectroscopy (EXAFS) at the vanadium, copper, and zinc K edge of $M_{0.25}V_2O_5$. The presence of zinc and copper allows the investigation of the zinc and copper K edges, which in turn reveals structural information about the neighborhood of the inserted metal. The combined study of the inserted metal and the vanadium gives additional details of the overall structure of the materials. Data analysis at the three different K edges is presented.

Figures 1 and 2 show the experimental EXAFS spectra of both Zn- and Cu-doped ARG-like samples as well as the k^2-extracted EXAFS signal and corresponding Fourier transform (FT). The two EXAFS signals are similar and are characterized basically by a smooth, simple oscillation. Also, at first glance the corresponding FTs display one main peak at a distance of about 1.8 Å. Because the FTs refer to the atomic distribution around the photoabsorber, it seems that in both compounds the metal ions have a similar atomic environment: the doping metal ion goes into a somewhat similar site. As to the structural nature of the site, there are two possible sites where a guest could be placed into the V_2O_5 host: between two bilayers or close to a single layer. The local geometry around the metal ion site is basically different in the two sites, and the EXAFS technique

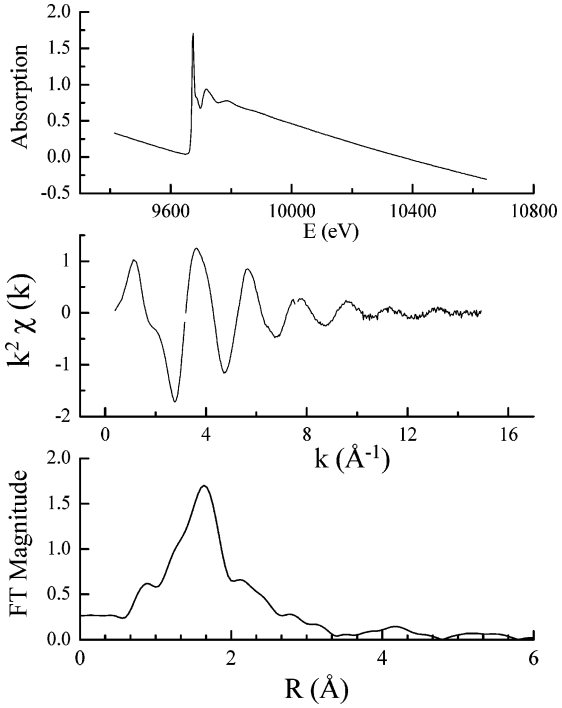

Figure 1. Preliminary data reduction of the Zn K-edge EXAFS spectrum of $Zn_{0.25}V_2O_5$ ARG-like material. The upper panel shows the raw EXAFS spectrum, the k^2-extracted EXAFS is reported in the middle panel, and the relative Fourier transform of the k^2-extracted EXAFS is displayed in the bottom panel.

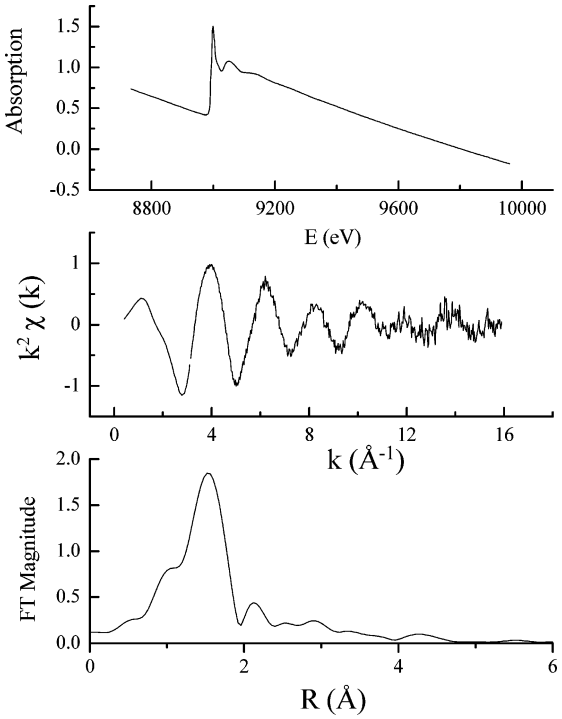

Figure 2. Preliminary data reduction of the Cu K-edge EXAFS spectrum of $Cu_{0.25}V_2O_5$ ARG-like material. The upper panel shows the raw EXAFS spectrum, the k^2-extracted EXAFS is reported in the middle panel, and the relative Fourier transform of the k^2-extracted EXAFS is displayed in the bottom panel.

should be definitive in choosing between the two. Briefly, if the metal occupies a site within a single bilayer, then the EXAFS spectra should characterized mainly by a first-shell peak due to the oxygen of the V_2O_5 sheet. The coordination number of the first shell would be 4. On the contrary, if the doping metal were between two bilayers, then the main contribution to the EXAFS spectra would be due to the linear configuration M−O−V that would generate a strong focusing effect. In this case, the coordination number of the first shell would be 2, and a strong second-shell M−V should appear.

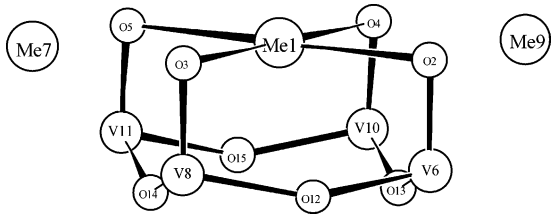

Figure 3. Ball-and-stick structure of the metal-doped V_2O_5 ARG-like materials. The numbering scheme used in the text is also shown. The metal atom (Me1) is 4-fold coordinated by apical oxygens, interacting with a single bilayer.

In light of this argument, we used a preliminary fitting procedure just to check the coordination number of the signal associated with the M−O first shell. The fitting procedure indicated a coordination number close to 4 for both compounds. Also, the inclusion of the linear term M−O−V produced very large residuals, indicating that the EXAFS signals is mainly due to the oxygen first shell. Hence, the structural model used in the calculation of the best fit is shown in Figure 3. The metal coordination site is centered among four vanadyl oxygens that belong to a single V_2O_5 bilayer. The metal is 4-coordinated by the apical oxygen of four VO_6 octahedra. The oxygens belong to the same V_2O_5 bilayer,[20] and the metal site is in a quasi-coplanar position with them. It is worth pointing out that the same model was used in the EXAFS analysis of a zinc-inserted V_2O_5 compound obtained via a different synthesis route.[12]

Because of the different local atomic environments, the three EXAFS best fits will be presented separately.

Zinc K Edge. Using the atomic label of Figure 3, the following two-atom contributions have been included in the fitting procedure: $\gamma^{(2)}$ $Zn_1-O_{2,3,4,5}$ (first shell) with a degeneracy of 4; $\gamma^{(2)}$ $Zn_1-O_{12,13,14,15}$ (second shell) with degeneracy of 4. In addition, a three-body contribution, $\eta^{(3)}$ Zn−O−V, has been added as well. It takes into account the four triplets $Zn_1-O_2-V_6$, $Zn_1-O_3-V_8$, $Zn_1-O_4-V_{10}$, and $Zn_1-O_5-V_{11}$, and the notation $\eta^{(3)}$ includes both $\gamma^{(2)}$ Zn−V and $\gamma^{(3)}$ Zn−O−V. The overall number of parameters included in the fitting procedure was 12: 3 bond distances, 1 asymmetry coefficient β, 1 angle, 4 EXAFS Debye−Waller factors, and 3 nonstructural terms (E_0, S_0^2, and the experimental resolution). E_0 is displaced a few electronvolts from the edge inflection point, 9661.8(4) eV, and S_0^2 is 0.85(2). The results of the fit are illustrated in Figures 4 and 5, panel a. Figure 4 shows the various contributions to the theoretical signal, and the comparison of the theoretical signal to the experimental one. Figure 5, panel a displays the relative FT. It is seen that the theoretical curve matches the experimental one very well in both figures, supporting the choice of the structural model and the accuracy of the analysis. It is clear that the first-shell contribution dominates the theoretical signal and that the inclusion of the Zn−Zn signal is not necessary.

The interatomic distances and the corresponding EXAFS Debye−Waller factors of the doped $Zn_{0.25}V_2O_5$ are shown in Table 1 with the associated errors. They were determined by the correlation maps (contour plot) for each pair of parameters. The estimated statistical error is associated with the 95% confidence interval.[27] The zinc site in the doped $Zn_{0.25}V_2O_5$ materials is found to be 4-fold coordinated by four oxygens at distance of about 2.06 Å. The oxygens belong to the same V_2O_5

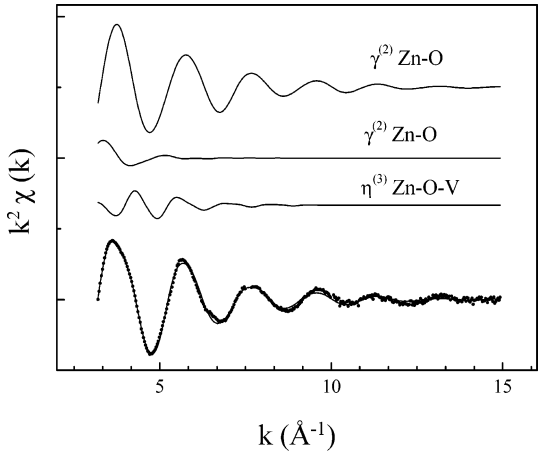

Figure 4. Details of the EXAFS analysis of the Zn K edge of the $Zn_{0.25}V_2O_5$ ARG-like material. Shown are the individual EXAFS contributions, in terms of two-body and three-body signals, to the total theoretical signal. At the bottom, the comparison of the total theoretical signal (−) with the experimental (• • •) is also illustrated.

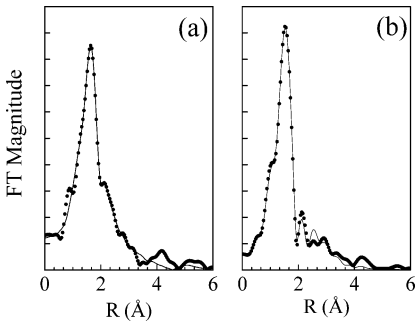

Figure 5. Comparison of the experimental (−) and theoretical (●−●) Fourier transform curves of k^2-extracted EXAFS taken at the Me K edge of the $Zn_{0.25}V_2O_5$ (panel a) and of the $Cu_{0.25}V_2O_5$ (panel b) ARG-like materials. The curves are obtained in the 3.1−15-Å^{-1} k space.

TABLE 1: EXAFS Best-Fitting Results of $Cu_{0.25}V_2O_5$ and $Zn_{0.25}V_2O_5$ Arg-Like Materials[a]

bond length (degeneracy) Debye−Waller	$Cu_{0.25}V_2O_5$ Arg-like	$Zn_{0.25}V_2O_5$ Arg-like	$Zn_{0.14}V_2O_5$ aerogel[b]
M−O/Å (4)	1.960(5)	2.065(3)	2.048(6)
σ^2/Å^2	0.005(1)	0.006(1)	0.0074(14)
β	0	0.10(5)	
M−O/Å (4)	2.268(7)	2.255(5)	2.28(1)
σ^2/Å^2	0.029(1)	0.037(3)	0.021(3)
V−O apical/Å (4)	1.67(2)	1.69(1)	
σ^2/Å^2	0.008(7)	0.015(2)	
M−V/Å[b]	2.78[c]	2.79[c]	
M−O−V/deg (4)	100(1)	96(1)	99(3)
σ^2_θ/deg^2	79(7)	49(4)	21(5)

[a] Metal edges. The estimated parameter errors are indicated in parentheses. [b] Data obtained from ref 12. [c] Data obtained from the three-body configuration (using angle M−O−V and distances V−O).

bilayer, and the metal site is in a quasi-coplanar position with them, describing an angle Zn−O−V of about 96°.

Table 1 also reports, for comparison, the relevant structural parameters found in the chemically inserted $Zn_{0.14}V_2O_5$ sample[12] obtained using a different synthesis route. In fact, the doped material described in the present paper was produced by mixing a selected stoichiometric amount of zinc powder, whereas the previous materials were made by reaction with dimethyl zinc (chemical intercalation).[5]

From the table it is seen that the number of structural parameters as well as the bond distances and angles are almost exactly the same, indicating that the zinc ion goes into the same site even though two different synthesis routes were used. Notwithstanding, we note a slightly lower Zn−O first-shell distance in the chemically inserted ARG as compared to that in the doped ARG-like material. We conclude that the two routes yield identical intercalation sites for zinc.

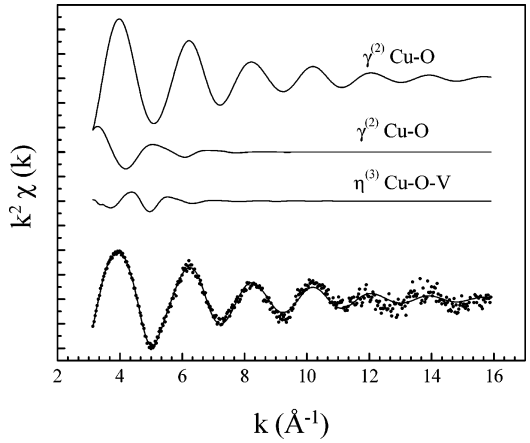

Figure 6. Details of the EXAFS analysis of the Cu K edge of the $Cu_{0.25}V_2O_5$ ARG-like material. Shown are the individual EXAFS contributions, in terms of two-body and three-body signals, to the total theoretical signal. At the bottom, the comparison of the total theoretical signal (−) with the experimental (• • •) is also illustrated.

Copper K Edge. The EXAFS best fit at the copper K edge was carried out using the same structural model as for the zinc system (see above). The multiple scattering paths for the fitting were calculated ab initio from the geometrical coordinates available from the zinc study when substituting copper for zinc species in the material.

As in the case of zinc, the atomic arrangement around copper is described by a few important paths: (a) first-shell $\gamma^{(2)}$ Cu−O (degeneracy 4); (b) second-shell $\gamma^{(2)}$ Cu−O_2 (degeneracy 4); and (c) the three-body contribution $\eta^{(3)}$ Cu−O−V with degeneracy 4. The overall number of parameters included in the fitting procedure was 12, including the structural terms and E_0, S_0^2, and the experimental resolution. E_0 is found to be 8976.3(8) eV, and S_0^2 is 0.85(5). This fitting approach yields the result illustrated in Figure 6, which compares the theoretical EXAFS signal with the experimental one. The single contributions, in terms of two- and three-body interactions, are shown in the upper section of the plot. As in the case of the zinc-doped ARG-like sample, the four-oxygen first shell represents the main signal, and the Cu−Cu contribution is negligible. That is, we conclude that the contribution of a two body Cu−Cu interaction is not significant in these samples. The total theoretical EXAFS signal accounts for the whole experimental spectrum. Figure 5, panel b shows the FT plot of the experimental and theoretical signals. The overlap between the curves is further support for the goodness-of-fit procedure and therefore of the structural model proposed. In Table 1 are listed the interatomic distances, the angles, and the corresponding EXAFS Debye−Waller factors as obtained from the best fit with the relative errors from the contour plots. The copper ion is coordinated by four apical oxygens of one bilayer. The Cu−O bond length for the first shell is shortened with respect to Zn−O, leading to a value of 1.96 Å. Copper occupies the same site as found for zinc.

Vanadium K Edge. Vanadium K-edge X-ray absorption spectra have also been recorded for both copper- and zinc-doped V_2O_5. Although the vanadium K edge in V_2O_5 intercalation materials is generally used for monitoring the vanadium oxidation state and the structural modifications of the vanadium environment upon lithium insertion, in our case it serves to give

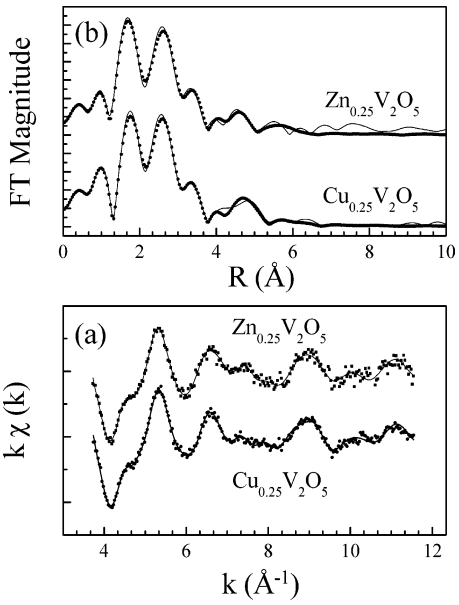

Figure 7. Best fit of the vanadium-edge EXAFS signals of $Cu_{0.25}V_2O_5$ and $Zn_{0.25}V_2O_5$ ARG-like materials. Shown is the comparison of the experimental (• • •) and theoretical (−) signals. Panel a displays the *k*-extracted EXAFS signals. Panel b shows the corresponding Fourier transforms obtained in the 3.5−12-Å^{-1} *k* space.

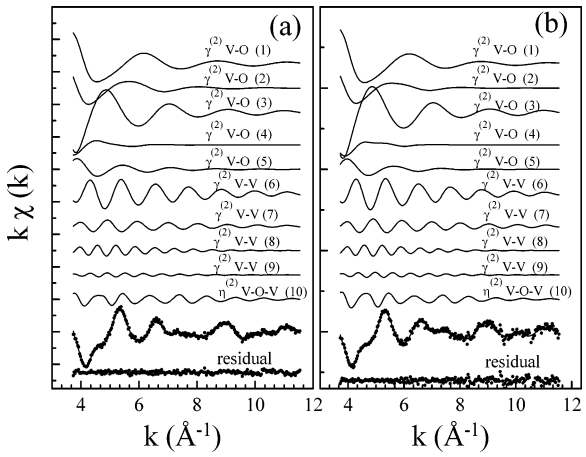

Figure 8. EXAFS analysis of the V K-edge spectra of $Cu_{0.25}V_2O_5$ (panel a) and $Zn_{0.25}V_2O_5$ (panel b) ARG-like materials. Shown is the individual EXAFS contributions, in terms of two-body and three-body signals, to the total theoretical signal. The numbering nomenclature is consistent with the associated parameters reported in Table 2. At the bottom is reported the comparison of the total theoretical signal (−) with the experimental (• • •), together with the residual curve.

complementary structural information for the two pristine compounds. Figure 7 shows the comparison of the theoretical and experimental EXAFS spectra (panel a) of $Cu_{0.25}V_2O_5$ and $Zn_{0.25}V_2O_5$ and the corresponding Fourier transforms (panel b). The EXAFS experimental signals are clearly the same and resemble those of a "V_2O_5 gel" (XRG or ARG). This suggests that the vanadium site is only slightly affected by the insertion of a dopant metal, especially when a small amount of doping metal is used. (In this case, the metal, M, is about $^1/_8$ of the vanadium.)

To verify this hypothesis, the vanadium K-edge EXAFS spectra were analyzed. The analysis of an EXAFS spectrum of a V_2O_5 gel is not simple because of the "characteristic" large asymmetry of the vanadium environment for the distances in the first shell. As pointed out by Stizza[28] and co-workers several years ago, the use of a natural polarization of a synchrotron radiation beam can be efficiently used because it permits one to separate experimentally the contributions of neighboring atoms in different directions. In a recent paper,[17] we pointed out that a polarized-EXAFS analysis of an oriented V_2O_5 XRG can be used to build up the fitting parameters for the analysis of the powder EXAFS spectrum, and we demonstrated that the two best fits are consistent (i.e., they yield the same outcome). In the present study, we have used the same fitting approach, extended this time to doped ARG-like materials. In particular, the structural parameters are allowed to float only to some extent, considering that they are close to that of ref 17. In this way, all of the structural parameters are constrained and consistent with those normally quoted for V_2O_5 gel compounds. This makes the EXAFS analysis reliable, even considering the relatively large number of two-body contributions (see below).

Figure 8 illustrates the details of the EXAFS analysis in terms of *n*-body contributions of $Cu_{0.25}V_2O_5$ (panel a) and $Zn_{0.25}V_2O_5$ (panel b). At the bottom, the comparison of the theoretical and experimental signals is also shown. From the plots, it is seen that the theoretical curves match well with the experimental ones. Also, from the residuals reported in the same figure, there is no sinusoidal signal, indicating that no other contributions are missing. In particular, the inclusion of the possible M−V interaction was not necessary. The following two-atom MS signals are included in the fitting procedure: the first five $\gamma^{(2)}$ signals are due to the vanadium first shell. All of these signals are rather important and they are characteristic of a particular V−O distance, so it is not possible to group them. In addition, another four $\gamma^{(2)}$ signals are generated by vanadium in the second and third shells. They are not directly connected to the photoabsorber by an oxygen bridge. Finally, the three-body $\eta^{(3)}$ terms due to the V−O−V triplet have been included. They also take into account the V−V distance of the triplet V−O−V. It is worth pointing out that all of the MS signals are necessary to determine the theoretical plot. Figure 7, panel b compares the FT plots of the experimental and theoretical signals: the curves match well in both $Cu_{0.25}V_2O_5$ and $Zn_{0.25}V_2O_5$, further supporting the reliability of the data analysis.

The fitting procedure was computed with 23 free parameters: 9 distances, 1 angle, and 10 Debye−Waller-like factors. The other three parameters were E_0 (which has been found to be 5474(1) and 5475(2) eV for $Cu_{0.25}V_2O_5$ and $Zn_{0.25}V_2O_5$, respectively[29]), S_0^2 (which is 0.81(8) and 0.87(9) for $Cu_{0.25}V_2O_5$ and $Zn_{0.25}V_2O_5$, respectively), and the experimental resolution. In the present discussion, the actual number of free parameters is lower because of the structural constraints mentioned above.

The degeneracy, the interatomic distances, and the corresponding EXAFS Debye−Waller factors of both samples obtained from the best fits are shown in Table 2 together with the structural data obtained by the EXAFS analysis of the pristine V_2O_5 ARG. The errors associated with the parameters obtained with the EXAFS analysis are indicated as well as in Table 2. All of the bond lengths are almost the same for the V_2O_5 ARG, $Cu_{0.25}V_2O_5$, and the $Zn_{0.25}V_2O_5$ ARG-like material. The V−O distances of the *xy* plane as well as the V···V interactions are just slightly shorter for the nondoped ARG sample. Basically, the symmetry around the vanadium site does not change much, but the dopant metal slightly modifies the symmetry, "attracting toward itself" the apical oxygens.

General Results. The number of equivalent sites available to the doping metal in the bilayer V_2O_5 structure would be filled when $x = 1$. In this context, the M−M interaction should appear at a distance of about 3.3 Å. Both metal K-edge analyses in the investigated compound (where $x = 0.25$) highlight the fact that the EXAFS contribution of the M−M interaction is not

TABLE 2: EXAFS Best-Fitting Results of $Cu_{0.25}V_2O_5$ and $Zn_{0.25}V_2O_5$ Arg-Like Materials

bond length (degeneracy) Debye−Waller	$Cu_{0.25}V_2O_5$	$Zn_{0.25}V_2O_5$	V_2O_5 aerogel[b]
(1) V−O_{apical} "up"/Å (1)	1.61(2)	1.60(2)	1.603(7)
σ^2/Å^2	0.003(2)	0.005(3)	0.061(15)
(2) V−O_{plane}/Å (1)	1.71(2)	1.72(2)	1.71(1)
σ^2/Å^2	0.009(6)	0.016(5)	0.019(2)
(3) V−O_{plane}/Å (2)	1.91(1)	1.90(1)	1.867(5)
σ^2/Å^2	0.004(1)	0.004(2)	0.011(1)
(4) V−O_{plane}/Å (1)	2.00(5)	2.04(3)	1.98(2)
σ^2/Å^2	0.031(8)	0.035(13)	0.017(5)
(5) V−O_{apical} "down"/ Å (1)	2.36(4)	2.38(6)	2.31(2)
σ^2/Å^2	0.008(6)	0.021(12)	0.008(5)
(6) V−V/Å (2)	3.08(1)	3.10(2)	3.08(1)
σ^2/Å^2	0.005(3)	0.005(3)	0.011(2)
(7) V−V/Å (1)	3.37(3)	3.38(4)	3.43(1)
σ^2/Å^2	0.005(4)	0.005(4)	0.016(2)
(8) V−V/Å (5)	5.06(5)	5.07(5)	
σ^2/Å^2	0.015(8)	0.018(8)	
(9) V−V/Å (2)	5.36(9)	5.3(1)	
σ^2/Å^2	0.012(10)	0.011(10)	
V−V/Å[c]	3.53[c]	3.52[c]	3.58[c]
(10) V−O−V/deg (2)	155(6)	155(5)	148(2)
σ^2_θ/deg^2	46(30)	79(40)	34(20)

[a] Vanadium edge. The estimated parameter errors are indicated in parentheses. The numbers in parentheses indicate the association with the theoretical signals displayed in Figure 8. [b] Data from ref 17. [c] Data obtained from the three-body configuration (using angle V−O−V and distances V−O).

observed, but this does not mean that the M−M interaction does not exist. In fact, when the metal doping level is increased above 0.25, the M−M contribution becomes progressively more significant, and its inclusion would be required. This contribution must also be taken into account when analyzing the vanadium K edge. As seen from Table 2, we did not include a M−V interaction to obtain a good fit, so it seems that there is no significant difference in the vanadium atomic environment for a doping amount of 0.25 compared to that of V_2O_5 ARG. Only this result is apparent and is due to the low stoichiometric ratio of copper (or zinc) to vanadium: there is only one copper (zinc) atom to every eight vanadium atoms. Therefore, the inclusion of a higher-shell M−V contribution would not improve the data analysis.

If we compare the results from Tables 1 and 2, an apparent contradiction appears: the V−O apical bond distance involved in the triplet M−O−V should give a contribution at both metal and V K edges. For example, considering the $Cu_{0.25}V_2O_5$ sample, the V−O apical bond length is quoted to be 1.61 Å from the fit at the vanadium K edge (V−O apical "up" of Table 2) and 1.67 Å from the fit at the copper K edge (V−O apical of Table 1). The apparent contradiction is resolved if we take account of the low stoichiometric ratio between copper and vanadium in the present study: not all of the vanadium sites are characterized by the triplet V−O−Cu because not all of the "preferred sites" are filled by copper ions. On the contrary, all of the copper sites involve Cu−O−V triplets. Therefore, we consider the copper EXAFS analysis to be definitive in revealing the local structure. This also reveals the advantage of recording EXAFS spectra at both K edges.

Discussion

The combined XAFS study at zinc and copper K edges in doped V_2O_5 ARG-like material has made possible a detailed investigation of different metal intercalation sites in the high-insertion-capacity host. This study proved that the preferred site for two metal ions in the vanadium oxide host is the same and is not influenced by the metal itself. The EXAFS analysis presented above has confirmed the tetracoordination of the metal in $M_{0.25}V_2O_5$ ARG-like compounds. In addition, the analysis has indicated that the coordinating oxygens belong to the same V_2O_5 layer. The results are consistent with the square-planar coordination geometry of the metal atom. The doping metals are in the same site. The proposed structure of the metal site in $M_{0.25}V_2O_5$ samples is shown in Figure 3. In addition, the structural data of two zinc-doped V_2O_5 compounds prepared via different synthesis routes yields the same picture: the zinc ions occupy the same site. A difference appears when the first-shell distances are compared: the Zn−O first-shell distance is found to be longer than those of a previous study.[12] Also, the M−O first-shell distance was shorter for copper than for zinc. M−O first-shell distances depend on the doping metal: a higher atomic number is related to a longer bond.

In the framework of the chemistry of intercalation of V_2O_5 gel materials, this paper supports two main conclusions. First, using different doping metal ions, we found that the preferred site remains the same and is retained when the same metal ion is inserted by two different synthesis routes. Second, we no longer have to refer to mobile or immobile sites. Thus, the basis of differences in the electrochemical behavior should be studied by looking at other characteristics, such as bond distances (Zn−O first-shell distance is longer in ARG-like than in ARG material) or structural disorder induced by the doping metal (see below).

The XAFS technique has been used to investigate the details of the short-range structure in this disordered system because it has a unique sensitivity.[30] A comparison of the copper- and zinc-doped V_2O_5 compounds may also be made with other aspects of the analysis. The specific parameters are the asymmetric coefficient β and the bond variance. As pointed out in the Experimental Section, to take into account the anharmonic effects of the first shell (M−O) due to structural disorder, we have used the Γ function, which leads to the Gaussian approximation when the asymmetric coefficient β approaches zero. From Table 1, it is seen that all of the bond variances (EXAFS Debye−Waller) found for $Zn_{0.25}V_2O_5$ are larger with respect to those found for $Cu_{0.25}V_2O_5$; in addition, the asymmetric coefficient β is 0.10(5) in the zinc-doped sample, and it approaches zero in the copper-doped V_2O_5. This remarkable increase in the bond variances, associated with the value of the asymmetry coefficient, is an indication of the larger structural disorder present in the $Zn_{0.25}V_2O_5$ material. Despite the occurrence of a similar atomic environment of the copper- and zinc-doped ARG-like samples, the structural disorder as well as the pertinent M−O first shell bond distance might play a key role in determining different electrochemical behavior.

An important consequence of the preferred site described in Figure 3, where the metal ions interact only with a single bilayer, is the possibility that the empty interlayer spacing is then available for further ion insertion. As an example, the reversibility of insertion/release cycles for lithium ions in the $Cu_{0.1}V_2O_5$ xerogel host is not surprising.[7] This cathode also shows a highly reversible formation of copper metal during the lithium insertion.[15] Experiments are in progress to characterize both the electrochemical capabilities and the structural and electronic reversibility in $Cu_{0.25}V_2O_5$ and $Zn_{0.25}V_2O_5$ ARG-like materials.

Conclusions

The present work has characterized the structure of copper- and zinc-doped V_2O_5 ARG-like materials. The use of a

synchrotron radiation source has revealed statistically significant XAS spectra at both vanadium and doping metal K edges. The experiments were performed at the Synchrotron Radiation Source (SRS) at Daresbury Laboratory, Warrington, England. The data analysis used a multiple scattering formalism.

The results reported here answer the question about the effects of the metal's atomic number on the preferred site using an accurate study of the zinc and copper neighborhoods. In both cases, the preferred doping-metal site is within a single V_2O_5 layer, 4-fold coordinated by the apical oxygen of four VO_6 octahedra. In addition, there is no evidence of a Cu−Cu or Zn−Zn contribution because only 25% of the sites are filled. The $M_{0.25}V_2O_5$ materials were synthesized by a direct doping process instead of chemical intercalation with an organometallic reagent. Both routes yield the same local atomic arrangement. This conclusion suggests that the metal coordination site centered among four vanadyl oxygens (the site of Figure 3) is the preferred one for the general class of compounds $M_xV_2O_5$ with $x \leq 0.25$. For instance, the combined analysis of the first-shell anharmonic contribution as well as the M−O bond variance gives evidence for higher structural disorder in zinc-doped samples as compared to that in copper samples.

This paper also provides rather complete structural information about the local atomic arrangement of the vanadium and doping-metal site. In both cases, there is no evidence for an M−M or V−M interaction. To understand the M−M and V−M interactions, an exhaustive XAS analysis on doped material with a higher amount x of the doping metal is in progress. These new studies may reveal other preferred sites inside the V_2O_5 structure.

Acknowledgment. We appreciate the support of the DOE under contract DE-FG02-01ER15221. Daresbury Laboratory and the European Community are kindly acknowledged for assistance during the XAFS experiments (EC grant no. 37102).

References and Notes

(1) Livage, J. *Coord. Chem. Rev.* **1998**, *178−180*, 999.
(2) Chirayil, T.; Zavalij, P. Y.; Whittingham, M. S. *Chem. Mater*. **1998**, *10*, 2629.
(3) Le, D. B.; Passerini, S.; Guo, J.; Ressler, J.; Owens, B. B.; Smyrl, W. H. *J. Electrochem. Soc*. **1996**, *143*, 2099.
(4) Passerini, S.; Le, D. B.; Smyrl, W. H.; Berrettoni, M.; Tossici, R.; Marassi, R.; Giorgetti, M. *Solid State Ionics* **1997**, *104*, 195.
(5) Le, D. B.; Passerini, S.; Coustier, F.; Guo, J.; Soderstrom, T.; Owens, B. B.; Smyrl, W. H. *Chem. Mater*. **1998**, *10*, 682.
(6) Coustier, F.; Hill, J.; Owens, B. B.; Passerini, S.; Smyrl, W. H. *J. Electrochem. Soc.* **1999**, *146*, 1355.
(7) Coustier, F.; Passerini, S.; Smyrl, W. H. *J. Electrochem. Soc.* **1998**, *145*, L73 .
(8) Coustier, F.; Le, J.-M.; Passerini, S.; Smyrl, W. H. *Solid State Ionics* **1999**, *116*, 279.
(9) Stallorworth, P. E.; Kostov, S.; denBoer, M. L.; Greenbaum, S.; Lampe-Onnerud, C. *J. Appl. Phys.* **1998**, *83*, 1247.
(10) Poumellec, B.; Kraizman, V.; Aifa, Y.; Cortes, R. *Phys. Rev. B* **1998**, *58*, 6133.
(11) Clinton, D. E.; Tryk, D. A.; Bae, I. T.; Urbach, F. L.; Antonio, M. R.; Scherson, D. A. *J. Phys. Chem.* **1996**, *100*, 18511.
(12) Giorgetti, M.; Passerini, S.; Smyrl, W. H.; Berrettoni, M. *Chem. Mater*. **1999**, *11*, 2257.
(13) Giorgetti, M.; Passerini, S.; Berrettoni, M.; Smyrl, W. H. *J. Synchrotron Radiat.* **1999**, *6*, 743.
(14) Giorgetti, M.; Passerini, S.; Smyrl, W. H.; Muckerjee, S.; Yang, X. Q.; McBreen, J. *J. Eletrochem. Soc*. **1999**, *146*, 2387.
(15) Giorgetti, M.; Mukerjee, S.; Passerini, S.; McBreen, J.; Smyrl, W. H. *J. Eletrochem. Soc.* **2001**, *148*, A768.
(16) Smyrl, W. H.; Passerini, S.; Giorgetti, M.; Coustier, F.; Fay, M. M.; Owens, B. B. *J. Power Sources* **2001**, *469*, 97−98.
(17) Giorgetti, M.; Berrettoni, M.; Passerini, S.; Smyrl, W. H. *Electrochim. Acta* **2002**, *47*, 3163.
(18) Filipponi, A.; Di Cicco, A.; Natoli, C. R. *Phys. Rev. B* **1995**, *52*, 15122.
(19) Filipponi, A.; Di Cicco, A. *Phys. Rev. B* **1995**, *52*, 15135.
(20) Giorgetti, M.; Passerini, S.; Smyrl, W. H.; Berrettoni, M. *Inorg. Chem.* **2000**, *39*, 1514.
(21) Hedin, L.; Lundvquist, B. I. *J. Phys. C* **1971**, *4*, 2064.
(22) Krause, M.; Oliver, J. H. *J. Phys. Chem. Ref. Data* **1979**, *8*, 329.
(23) Filipponi, A. *J. Phys.: Condens. Matter* **1994**, *6*, 8415.
(24) Filipponi, A.; Di Cicco, A. *Task Quarterly* **2000**, *4*, 575.
(25) D'Angelo, P.; Di Nola, A.; Filipponi, A.; Pavel, N. V.; Roccatano, D. *J. Chem. Phys.* **1994**, *100*, 985.
(26) Filipponi, A.; Di Cicco, A. *Phys. Rev B* **1995**, *51*, 12322.
(27) Filipponi, A. *J. Phys.: Condens. Matter* **1995**, *7*, 9343.
(28) Stizza, S.; Mancini, G.; Benfatto, M.; Natoli, C. R.; Garcia, J.; Bianconi, A. *Phys. Rev B* **1989**, *40*, 12229.
(29) The values of the E_0s that we found appear to be far from the tabulated experimental value of the vanadium K-edge (5565 eV). The discrepancy is due to the large-intensity pre-edge peak of the V_2O_5 compounds that shortens (by about 10 eV) the first-derivative peak position of the spectrum (definition of E_0). Indeed, the E_0s that we found are consistent with the edge inflection point (at about 5578 eV in the investigated compounds).
(30) Filipponi, A. *J. Phys.: Condens. Matter* **2001**, *13*, R23.